Water Air Soil Pollut (2014) 225:1925
DOI 10.1007/s11270-014-1925-x

Modeling Carbon Stocks in a Secondary Tropical Dry Forest in the Yucatan Peninsula, Mexico

Zhaohua Dai · Richard A. Birdsey · Kristofer D. Johnson · Juan Manuel Dupuy · Jose Luis Hernandez-Stefanoni · Karen Richardson

Received: 17 October 2013 / Accepted: 4 March 2014 / Published online: 20 March 2014
© Springer International Publishing Switzerland 2014

Abstract The carbon balance of secondary dry tropical forests of Mexico's Yucatan Peninsula is sensitive to human and natural disturbances and climate change. The spatially explicit process model Forest-DeNitrification-DeComposition (DNDC) was used to estimate forest carbon dynamics in this region, including the effects of disturbance on carbon stocks. Model evaluation using observations from 276 sample plots in a tropical dry forest in the Yucatan Peninsula indicated that Forest-DNDC can be used to simulate carbon stocks for this forest with good model performance efficiency. The simulated spatial variability in carbon stocks was large, ranging from 5 to 115 Mg carbon (C)ha^{-1}, with a mean of 56.6 Mg C ha^{-1}. Carbon stocks in the forest were largely influenced by human disturbances between 1985 and 2010. Based on a comparison of the simulations with and without disturbances, carbon storage in the year 2012 with disturbance was 3.2 Mg C ha^{-1}, lower on average than without disturbance. The difference over the whole study area was 154.7 Gg C, or an 8.5 % decrease. There were substantial differences in carbon stocks simulated at individual sample plots, compared to spatially modeled outputs (200 m^2 plots vs. polygon simulation units) at some locations due to differences in vegetation class, stand age, and soil conditions at different resolutions. However, the difference in the regional mean of carbon stocks between plot-level simulation and spatial output was small. Soil CO_2 and N_2O fluxes varied spatially; both fluxes increased with increasing precipitation, and soil CO_2 also increased with an increase in biomass. The modeled spatial variability in CH_4 uptake by soils was small, and the flux was not correlated with precipitation. The net ecosystem exchange (NEE) and net primary production (NPP) were nonlinearly correlated with stand age. Similar to the carbon stock simulations, different resolutions resulted in some differences in NEE and NPP, but the spatial means were similar.

Keywords Biomass · Forest-DNDC · Greenhouse gas · Disturbance · Tropical dry forest

Z. Dai (✉) · R. A. Birdsey · K. D. Johnson
USDA Forest Service, 11 Campus Blvd, Suite 200, Newtown Square, PA 19073, USA
e-mail: zdai@fs.fed.us

Z. Dai · K. Richardson
Commission for Environmental Cooperation of North America, 393 rue St-Jacques Ouest, bureau 200, Montreal, QC H2Y 1N9, Canada

J. M. Dupuy · J. L. Hernandez-Stefanoni
Centro de Investigación Científica de Yucatán A.C, Unidad de Recursos Naturales, Calle 43# 130. Colonia Chuburná de Hidalgo, 97200 Mérida, Yucatán, Mexico

1 Introduction

Carbon (C) sequestration in forest ecosystems, including secondary tropical dry forests, is an important constituent of the terrestrial C sink that contributes to reducing the concentration of CO_2 in the atmosphere (Trettin et al. 2006; Miehle et al. 2006; Birdsey et al.

2007; Ryan 2008; Pan et al. 2011; Charman et al. 2013). Carbon sequestration in forests can be impacted by changes in surface air temperature, which has increased by 0.8 °C in the last hundred years (Hansen et al. 2006; IPCC 2007), and is now increasing at a rate of 0.2 °C per decade (IPCC 2007). Warming temperature is widely viewed to be the result of increasing emissions of greenhouse gases (GHG) such as CO_2 from human activities, primarily related to deforestation and fossil fuel consumption. On the other hand, conversion of croplands to forests and regeneration after deforestation may help regulate global CO_2 concentrations by maintaining or increasing the terrestrial C sink. Accordingly, understanding carbon dynamics in tropical dry forest ecosystems, especially secondary ecosystems, is critical not only to assess the role of forests in mitigating global warming but also to inform forest management decisions (Birdsey et al. 2006).

There is also a need to assess how the C dynamics of tropical dry forest ecosystems may respond to climate change. Accumulation and consumption of C in forest ecosystems is strongly related to soil moisture, which is regulated by precipitation and temperature (Pietsch et al. 2003; Riveros-Iregui and McGlynn 2009; Pacific et al. 2009). Changes in temperature and/or precipitation influence the forest soil moisture regime (Dai et al. 2011) and drive C dynamics in forest ecosystems (Raich and Schlesinger 1992), especially in tropical dry forest ecosystems where precipitation is less than potential evapotranspiration (Holdridge 1967; Borchert et al. 2002; Bauer-Gottwein et al. 2011). Furthermore, secondary tropical dry forests may be more sensitive to climate change and anthropogenic disturbances than humid tropical forests (Hodell et al. 1995; Kennard et al. 2002; Haug et al. 2003).

Many studies on C dynamics in tropical forests, including observations and simulations using various C models, have been conducted in the last several decades (Bianchini et al. 2001; Kato et al. 2013). However, C dynamics in secondary tropical dry forests has received less attention than other tropical ecosystems (Dupuy et al. 2012). There are substantial differences in forest structure, composition, and environmental conditions between tropical wet and dry forests although air temperature and soils may be similar. Many evergreen species in tropical wet forests can become deciduous or semi-deciduous in tropical dry forests and grow slowly due to water stress during the dry season (Daubenmire 1972). In summary, tropical dry forests are substantially different from tropical wet forests not only in species diversity but also in C accumulation and consumption.

The objectives of this study were threefold: (1) to evaluate and validate a spatially explicit biogeochemical model Forest-DeNitrification-DeComposition (DNDC) using biomass observation from 276 plots (Hernandez-Stefanoni et al. 2011; Dupuy et al. 2012) within a tropical dry forest at Kaxil Kiuic in the Yucatan Peninsula in Mexico, (2) to assess the effect of disturbances on C stocks, and (3) to estimate long-term dynamics of C sequestration in this tropical dry forest.

2 Methods and Data

2.1 Study Area

The study area is a tropical dry semi-deciduous forest landscape, about 350 km^2, centrally located in the Yucatan Peninsula, Mexico (20.02°–20.16° N, 89.60°–89.39° W) (Fig. 1), mainly comprised of forestlands (94 % of the area), with some croplands (about 5.35 %) and urban areas (about 0.75 %; Fig. 2). Swidden agriculture has been the historical land use in this area for over a thousand years (Rico-Gray and Garcia-Franco, 1991; Turner et al. 2001; Hernandez-Stefanoni et al. 2011; Dupuy et al. 2012). The current forest is a secondary regrowth after abandonment of croplands and after degradation due to harvesting of wood products.

The landscape topography consists of mosaics of low and moderate hills and small flat areas. Slope ranges from 0 to 90 %, with an average of 7 %. The elevation varies from 0 to 176 m above mean sea level, with a mean of 116 m. The climate is tropical, with a summer rain period from June to October and a dry season between November and May. The mean annual precipitation during the 38-year period from 1970 to 2007 was less than 1,200 mm, based on the climate data observed at five weather stations around Kaxil Kiuic. The mean temperature is 26.5 °C in this 38-year period (CONAGUA 2012).

The soil developed on limestone and is approximately neutral; pH ranges from 5.48 to 7.84 within the study area, with a mean of 7.22, based on soil samples analysis (Dupuy et al. 2012). Clay content varies considerably (20.7–84.0 %) in rock-free soil, with a mean of 49.0 %. The main soil types range from sandy clay to clay, but a few soils are loam. The stone content in most soils is high; visually estimated rock content is between 0 and

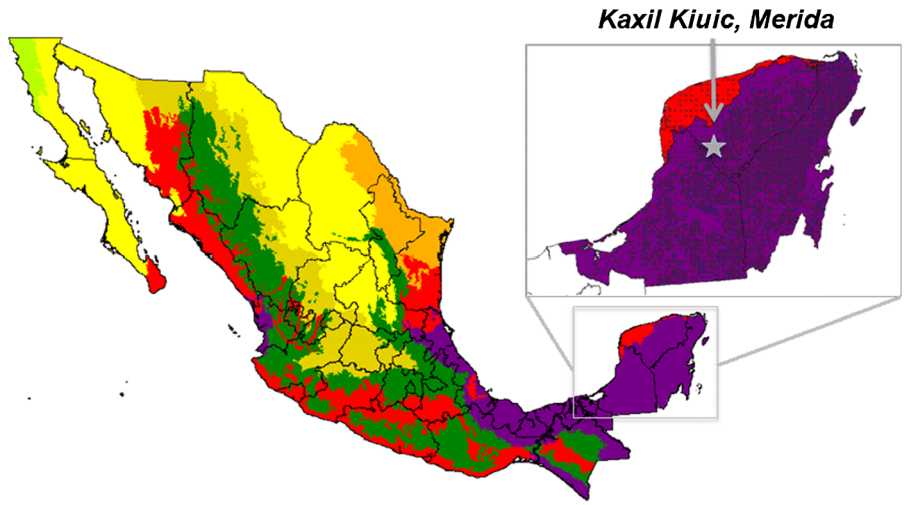

Fig. 1 Kaxil Kiuic forest in the Yucatan Peninsula, Mexico

90 %, with an average of 29 %; rock-free soil is rare in this region. Soil organic matter (SOM) ranges from 2.54 to 72.0 % in rock-free soil, with a mean of 23 % (Dupuy et al. 2012).

Vegetation in the forest area is regenerated after deforestation/degradation or cropland abandonment. An inventory of 276 plots was conducted in 2008–2009 (Hernandez-Stefanoni et al. 2011); most study sites were 7–74 years old in 2012, the mean age was 27. Stem density of woody plants ≥1 cm in diameter at breast height (DBH 1.3 m) varies widely (2,550–24,550) with a mean of 11,165 individuals ha^{-1}, density of trees 1≤DBH≤5 cm was 1,400–24,000 with a mean of 9,511 individuals ha^{-1}, and density of trees >5 cm in DBH was 0–4,950 with an average of 1,654 stems ha^{-1}. Plant species richness in this study area is relatively high, although it may be lower than the richness in humid tropical forests in Mexico. There were 123 species of trees >5 cm in DBH, and 41 species of trees 1–5 cm in 2008–2009. The canopy structure and main species have been reported by Hernandez-Stefanoni et al. (2011) and Dupuy et al. (2012).

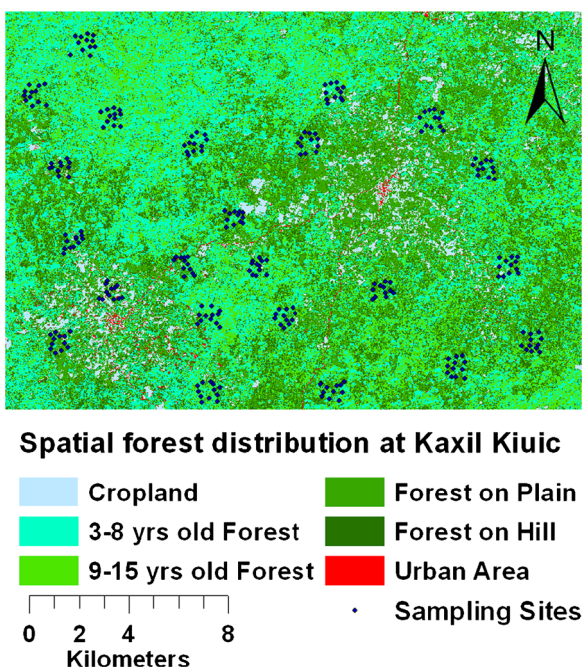

Fig. 2 Measurement sites for biomass and soils, and vegetation distribution in 2005 derived from a SPOT 5 satellite image of January 2005 (Hernandez-Stefanoni et al. 2011). *yrs* years

2.2 Field Measurements and Data Collection

Biomass was measured using 276 circular plots over a 350-km^2 area to estimate C stocks in this forest (Fig. 2) (Hernandez-Stefanoni et al. 2011). Twenty-three landscape units were delineated for measurements in order to account for the whole range of forest fragmentation and to evaluate the influence of landscape structure on species richness and biomass in this forest landscape (Hernandez-Stefanoni et al. 2011). The size of each landscape unit was about 1 km^2, in which 12 plots were installed using a stratified sampling design to represent different secondary forest cover classes. Tree height (TH, m) was measured using a graduated telescopic pole, and diameter at breast height (DBH, cm) was measured using standard diameter tapes (Hernandez-Stefanoni et al. 2011). Plot size was 200 m^2 to estimate

the biomass for trees >5 cm in DBH, and a 50-m^2 subplot within the 200-m^2 plot was designed to measure TH and DBH of trees 1≤DBH≤5 cm (Hernandez-Stefanoni et al. 2011). Biomass was estimated using the equations developed by Hughes et al. (1999) and Cairns et al. (2003) for trees <10 cm and ≥10 cm in DBH, respectively. The total biomass for each plot was integrated from the different measurements and reported as megagrams per hectare. Stand age of each of the inventoried forest plots was estimated by interviewing the land owners or users, especially those who were ≥40 years old (Hernandez-Stefanoni et al. 2011).

Soil samples were collected from each inventory plot. Three 10-cm-deep soil samples were collected from each plot at the center and at the northern and southern edges. Soil organic matter (SOM), pH, and texture were analyzed (Dupuy et al. 2012).

Climate data, including daily minimum and maximum temperature and daily precipitation, were available from six weather stations. Five of the stations were located near the study area, with data available from 1969 to 2007. One station is located in the study site and has collected data since 2006. Because of missing data for different times at different stations, the data were integrated into one composite dataset for a 43-year period from 1970 to 2012 for this study.

2.3 Spatial Data for Vegetation and Soil

The spatial distribution of vegetation was derived from the SPOT 5 satellite image of January 2005, created by Hernandez-Stefanoni et al. (2011). However, maps of stand age for the entire study area are not available, and the age varies spatially due to disturbances and land use change, including wood product harvest and abandonment of cropland. Because stand age is an important parameter to estimate the spatial distribution of C stocks using a modeling approach, stand age measurements from the 276 plots were spatially interpolated with a kriging method at 30-m resolution (Li and Heap 2008; Jassim and Altaany 2013). Soil parameters, including soil texture and SOM, were derived from field data (Dupuy et al. 2012). The maps of vegetation type, soil condition, and stand age were prepared at 30-m resolution. The vegetation map was converted from raster to polygons based on the vegetation classes to produce simulation units with distinct biophysiochemical characteristics for the spatially explicit model. The polygon size ranged from 0.0576 to 746.7 ha, with a mean of 1.17 ha. The maps of stand age and soil condition were combined with vegetation type as spatially explicit model inputs.

2.4 Disturbances

A map showing year of recent disturbances (unpublished, see "Acknowledgments") for the period 1985 to 2010 was created from Landsat scenes using a forest disturbance detection approach (Goward et al. 2008) (Fig. 3). The disturbance types were determined by comparing the disturbance map with the vegetation map (Fig. 2) derived from the SPOT 5 satellite image. We assumed that the disturbances that occurred between 1985 and 2010 were mainly due to land use change, including urbanization and the conversion of lands from forests to crops (mostly swidden agriculture), as well as agricultural abandonment. Three disturbance types, deforestation to agriculture or urban land use, agricultural abandonment, and forest product harvest, were identified to model the effects of disturbances on C stocks. If the vegetation map showed the disturbed lands as forestlands at present and the disturbance map did not show the lands as persistent forests, the disturbed lands were considered as secondary forests regenerated after agricultural abandonment. However, if the disturbance map showed the lands as persistent forests with perturbations and the vegetation map showed the lands as forests at present, we assumed that the disturbances were due to forest product harvests, and the forests regenerated after the deforestation or degradation. The remaining disturbances were forest conversion to agriculture or urban areas.

2.5 Model Setup and Validation

The biogeochemical model Forest-DNDC (Li et al. 2000; Stange et al. 2000) with a spatially explicit modeling approach (Dai et al. 2012) was used to estimate spatiotemporal C dynamics for this tropical dry semideciduous forest. The model is process-based, employed to simulate forest growth and C and N dynamics in forest ecosystems, including trace gas emissions, based on the balance of water, light, and nutrition in forest ecosystems (Li et al. 2000; Stange et al. 2000; Miehle et al. 2006). The model integrates photosynthesis, decomposition, nitrification-denitrification, carbon storage and consumption, and hydrothermal balance in forest ecosystems. The vegetation is divided into three layers:

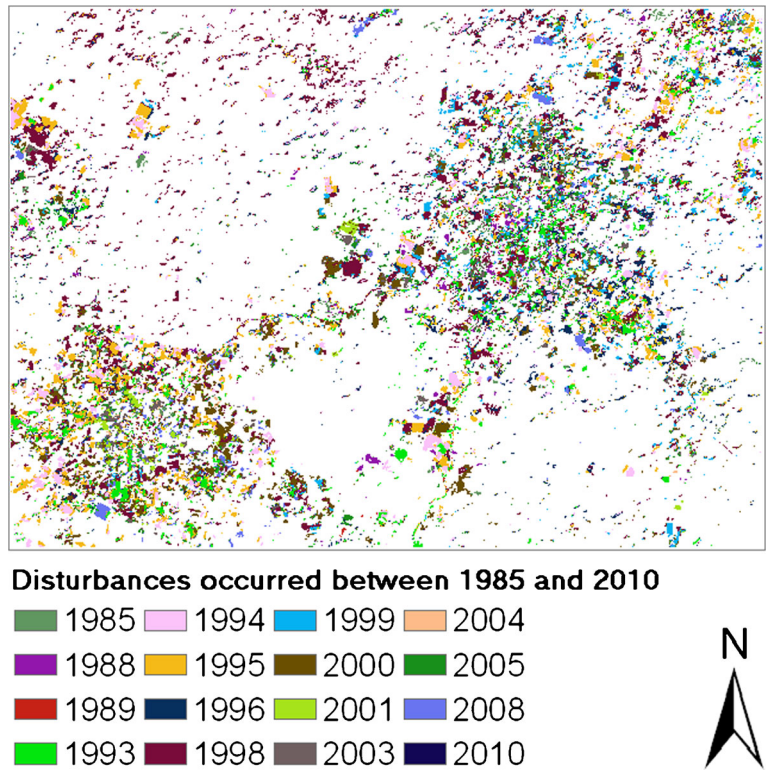

Fig. 3 Disturbances occurred in Kaxil Kiuic forest between 1985 and 2010

overstory, understory, and ground-growth. The vegetation of each layer is simulated based on competition for energy and nutrients. This model has been tested and used for estimating GHG from forested wetland and upland ecosystems and for assessing C sequestration in forests in a wide range of climatic regions, from boreal to tropical (Stange et al. 2000; Zhang et al. 2002; Li et al. 2004; Kiese et al. 2005; Kesik et al. 2006; Kurbatova et al. 2008; Dai et al. 2012). The main parameters for modeling C dynamics in this forested terrain are presented in Table 1.

The model was set up to simulate spatial C stocks for the Kaxil Kiuic forest and validated using biomass observations from the 276 plots within the forest. The model performance was evaluated with four widely used quantitative methods (Dai et al. 2011), i.e., the coefficient of determination (R^2, squared correlation coefficient), model performance efficiency (E) (Nash and Sutcliffe 1970), percent bias (PBIAS), and the RRS [the ratio of the root mean squared error (RMSE) to SD (standard deviation)] (Moriasi et al. 2007).

E ($-\infty$, 1) is the key variable used to evaluate the model performance and is calculated as

$$E = 1 - \frac{\sum (O_i - P_i)^2}{\sum \left(O_i - \overline{O}\right)^2} \quad (1)$$

where O_i, $\overline{O}$, and P_i are observed values, observation mean, and simulated results, respectively. The other evaluation variables, PBIAS and RRS, are computed, respectively, as

$$\mathrm{PBIAS} = \frac{\sum (O_i - P_i)}{\sum O_i} \times 100 \quad (2)$$

$$\mathrm{RRS} = \frac{\mathrm{RMSE}}{\mathrm{SD}} \quad (3)$$

where SD is the observed standard deviation; RMSE is the root mean squared error between observed and simulated values, the equation is

$$\mathrm{RMSE} = \sqrt{\frac{\sum (O_i - P_i)^2}{n}} \quad (4)$$

Table 1 Key vegetation and soil parameters for Forest-DNDC

Parameter	Parameter
Initial leaf N (%)	Leaf start TDD
AmaxA (mol g^{-1} s^{-1})	Wood start TDD
AmaxB	Leaf end TDD
Optimum photosynthetic temperature (°C)	Wood end TDD
Minimum photosynthetic temperature (°C)	Leaf N retranslocation
Amax fraction	Senescence start day
Growth respiration fraction	Leaf C/N
Dark respiration fraction	Wood C/N
Wood maintain respiration fraction	Leaf retention years
Root maintain respiration fraction	C reserve fraction
Light half saturation constant	C fraction of dry matter
Respiration Q10	Specific leaf weight (g m^{-2})
Canopy light attenuation	Minimum wood/leaf
Water use efficiency	Leaf geometry
DVPD1	Maximum N storage (kg N ha^{-1})
DVPD2	Maximum wood growth rate
Maximum leaf growth rate (% yr^{-1})	Coefficient of stem density (0–1)[a]
Spatial soil, climate, vegetation, and hydraulic parameters	
Soil organic carbon (%)	Hydraulic Conductivities (cm hr^{-1})
pH	Wilting point (0–1)
Clay (%)	Capacity (0–1)
Soil depth (cm, ≤150 cm)	Porosity (0–1)
Overstory species	Overstory age
Understory species	Understory age
Ground-growth (sedge and moss)	Daily minimum temperature (°C)
Daily maximum temperature (°C)	Daily precipitation (mm)

The meaning and description of these parameters are in the manual (http://www.dndc.sr. unh.edu)

[a] Usually, the coefficient of stem density is the ratio of forest to the bare (non-forest) areas in each simulating unit, and from 0 to 1

where n is the number of samples or the pairs of the observed and simulated values.

2.6 Model Application

After validation, Forest-DNDC was used to simulate current spatial C stocks to assess the effect of disturbances on C stocks and to estimate long-term C dynamics in the forest. The model was run for a 75-year period, starting from 1938, 1 year before the oldest trees regenerated in the forest, to assess C stocks, including the effect of disturbances. Because there was no available climate data for the period 1938 to 1969, we used the data from 1970 to 2002 in place of the missing data for the earlier period.

To assess long-term C dynamics in this forest, the model was run for a 150-year period. Similar to the simulation for assessing C stocks, the 75-year climate dataset was repeated for the 150-year period. The bases of the simulation time span are that (1) the oldest tree in this forest was 75 years old in 2012 based on the inventory (Hernandez-Stefanoni et al. 2011) due to land use change and forest product harvest, (2) secondary tropical dry forests in the Yucatan Peninsula may take ≥50 years to become mature after regeneration (Brown and Lugo 1982, 1990; Eaton and Lawrence 2008), and (3) the secondary forests regenerated from cropland conversion may take longer to recover biomass to the level of mature forests (Read and Lawrence 2003). Therefore, a 150-year simulation period was deemed necessary to cover the entire succession period of the forest.

3 Results and Discussion

3.1 Model Evaluation

The results from the model validation using biomass measurements from the 276 plots are presented in Fig. 4a and Table 2. The coefficient of determination (R^2=0.83) (Fig.4a) and means from observations (46.86 Mg C ha^{-1}) and simulation (46.92 Mg C ha^{-1}) showed that the aboveground biomass simulated by Forest-DNDC for the forest at Kaxil Kiuic was in good agreement with the measurements, with a reasonable slope (b=1.03) of the regression model between observed and simulated values, which is approximately 1.0, and an intercept (a=−1.33 Mg C ha^{-1}) that differs by only 2.8 % from the observed average. The PBIAS and RRS are −0.14 % and 0.46, respectively, within the ranges of satisfactory rating values (PBIAS ±25 %, RRS ≤0.7) (Moriasi et al. 2007). The model performance efficiency (E=0.79) is within the range of "very good" model performance rating (0.75≤E≤1.0).

The small divergence between observation and simulation may result from two sources of error. One is the error in the stand age estimated by interviewing local

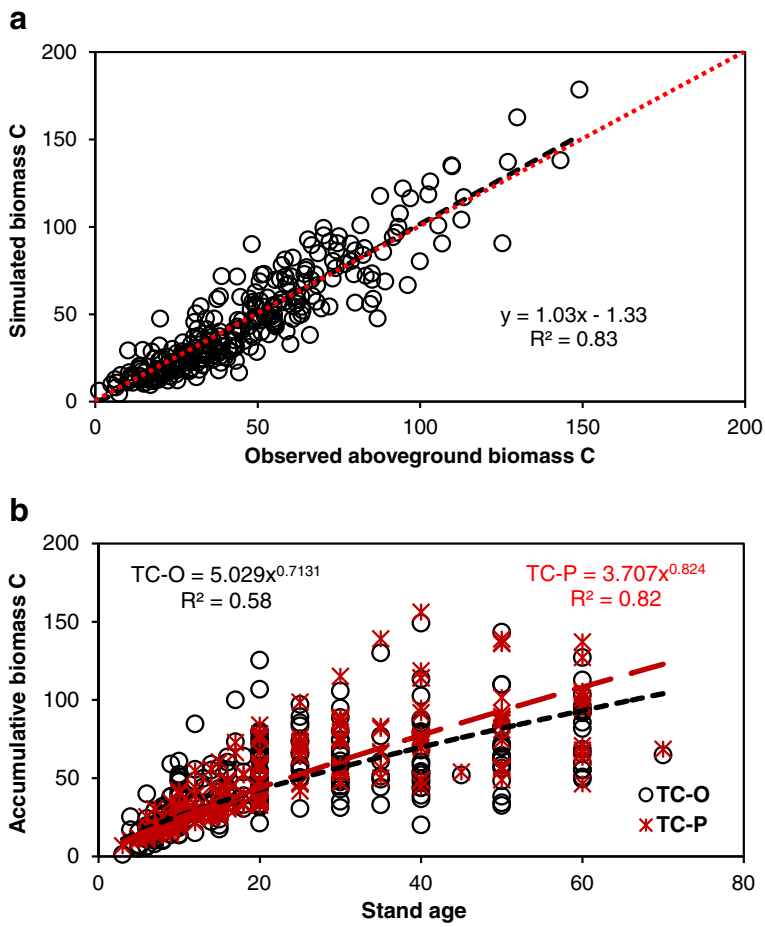

Fig. 4 **a** The total aboveground wood biomass C (Mg ha^{-1}) observed vs. simulated for the 276 plots in the tropical dry forest at Kaxil Kiuic in Yucatan Peninsula, Mexico. **b** The simulated (TC-P) and observed (TC-O) relationship between stand age (years) and the aboveground biomass (Mg C ha^{-1}) from the 276 plots in Kaxil Kiuic forest

people (Hernandez-Stefanoni et al. 2011). If stand age at a sample plot was substantially overestimated or underestimated, a large error in biomass estimated by the model might occur. For example, the observed biomass for plot 1303 was 125.32 Mg C ha^{-1} (about 250 Mg dry matter ha^{-1}) in 2008, and the estimated stand age was 20 years (Fig. 4b). Accordingly, the estimated average annual biomass growth rate would be more than 12 Mg yr^{-1} across the 20-year period on the basis of the stand age and biomass inventoried for the plot. Considering that this is a tropical dry semi-deciduous forest, with a long dry season of about 6 months from November to May, and where precipitation is less than potential evapotranspiration (Bauer-Gottwein et al. 2011), it is unlikely that this forest would have such a sustained high growth rate over the period.

The other source of error is the size of the observation plots, 50 and 200 m^2 for woody plants ≤5 cm and trees >5 cm in DBH, respectively. These plot sizes might be too small to provide a representative mean for estimating the correct biomass, especially the plot size (50 m^2) used to estimate the biomass for the trees ≤5 cm in DBH, because of high heterogeneity in their stem density,

Table 2 Results from model performance evaluation

Variable	Value	Variable	Value
Observed biomass (Mg C ha^{-1})	46.86	R^2	0.83
Simulated biomass (Mg C ha^{-1})	46.92	*E*	0.79
Observed SD (Mg C ha^{-1})	27.43	PBIAS	−0.14
Simulated SD (Mg C ha^{-1})	30.94	RRS	0.46
Slope	1.03	Intercept	1.33

SD standard deviation, R^2 coefficient of determination, *E* model performance efficiency, *PBIAS* percent bias, *RRS* ratio of RMSE to SD (see Model Setup and Parameterization); *slope* and *intercept* slope and intercept of the regression model between observations and simulation, respectively

ranging from 1,400 to 24,000 individuals per hectare. The small trees were important contributors to the total biomass for some plots.

Since all four model evaluation variables consistently indicated that the model works well for this hilly forest landscape, the model was used to assess C dynamics for the forest at Kaxil Kiuic and similar forests in The Yucatan peninsula.

3.2 Spatial Difference in Aboveground Biomass

Aboveground biomass C was simulated for the entire region using polygons converted from 30-m resolution maps. The simulated C stocks for 2012 are presented in Fig. 5. There was considerable variability in forest biomass C (i.e., urban and crop areas excluded), ranging from 5.0 to 115.0 Mg C ha^{-1}, with a mean of 56.6 Mg C ha^{-1}. The spatial difference in aboveground biomass C is mainly related to differences in stand age (Hernandez-Stefanoni et al. 2011; Dupuy et al. 2012), which are primarily the result of recent land use changes. When the results from the polygon-based simulation were compared to simulations using the 276 plots, the overall averages from the 276 plots (53.2 Mg ha^{-1} for 2012) and polygons (56.6 Mg C ha^{-1} in 2012) were similar. However, there was a substantial difference in aboveground biomass at some locations. For example, at plot 106 the simulated polygonal aboveground biomass was 113.7 Mg C ha^{-1}, but the value using the plot data was 143.2 Mg C ha^{-1} in 2008, and the observed biomass was 149.0 Mg C ha^{-1} in 2008. The discrepancy between the two simulations might be the result of errors in estimated stand age and boundaries of simulation units which may not exactly correspond with the sampling area.

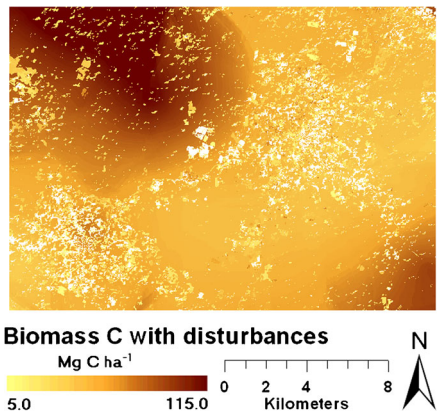

Fig. 5 Spatial distribution of estimated biomass (Mg C ha^{-1}) for 2012 in Kaxil Kiuic forest with disturbances occurred between 1985 and 2010; the blank (white) spots are agricultural and urban areas

There are differences between the interpolated stand age and the field data obtained by interviewing local people. For example, the field-estimated stand age for plot 106 was 40 years, compared to 30 years obtained from the interpolated map. This was due to one nearest neighbor plot being only 7 years old. Similarly, the SPOT-derived vegetation characteristics and soil condition could be spatially incongruent with the plot measurements because the polygon size, which ranged from 0.0576 to 746.7 ha, was much larger than the plot size, 0.02 ha. Since the regional averages simulated using plots and polygons were similar and consistent, we suggest that stand age interpolated from inventoried plot data and combined with coarse vegetation and soil conditions can be used to assess regional C stocks. Yet, errors related to the resolution issues raised above may result in under- or overestimation of C stocks at some specific locations, which should be considered if the outputs are used at small scales to inform landscape-scale management plans.

3.3 Soil CO_2 Flux

The spatial distribution of soil CO_2 flux at Kaxil Kiuic varied considerably as indicated by Fig. 6a which shows the simulated flux for the 276 plots in 2012. The flux ranged from 1.06 to 3.46 Mg C ha^{-1} year^{-1}, with an arithmetic mean of 2.37 Mg C ha^{-1} year^{-1} and median of 2.31 Mg C ha^{-1} year^{-1}. The small difference between the arithmetic mean and the median of soil CO_2 flux suggests that its spatial distribution was normal in this landscape. The variability of soil CO_2 flux is related to spatial differences in soil and vegetation, especially vegetation, because its distribution is heterogeneous in space leading to spatial differences in heterotrophic respiration, root respiration, and organic matter decomposition associated with dead trees, root mass, and litter produced by natural and anthropogenic factors.

Annual soil CO_2 flux from plot 407 for the period 1970 to 2012 is an example in which the flux increased linearly and significantly ($P<0.01$) at a rate of 22.2 kg C ha^{-1} year^{-1} over the 43-year period from 1970 to 2012 (Fig. 6b). This increase may be associated with tree growth accompanied by soil respiration, including root respiration. Root mass increased from 4.23 Mg C ha^{-1}

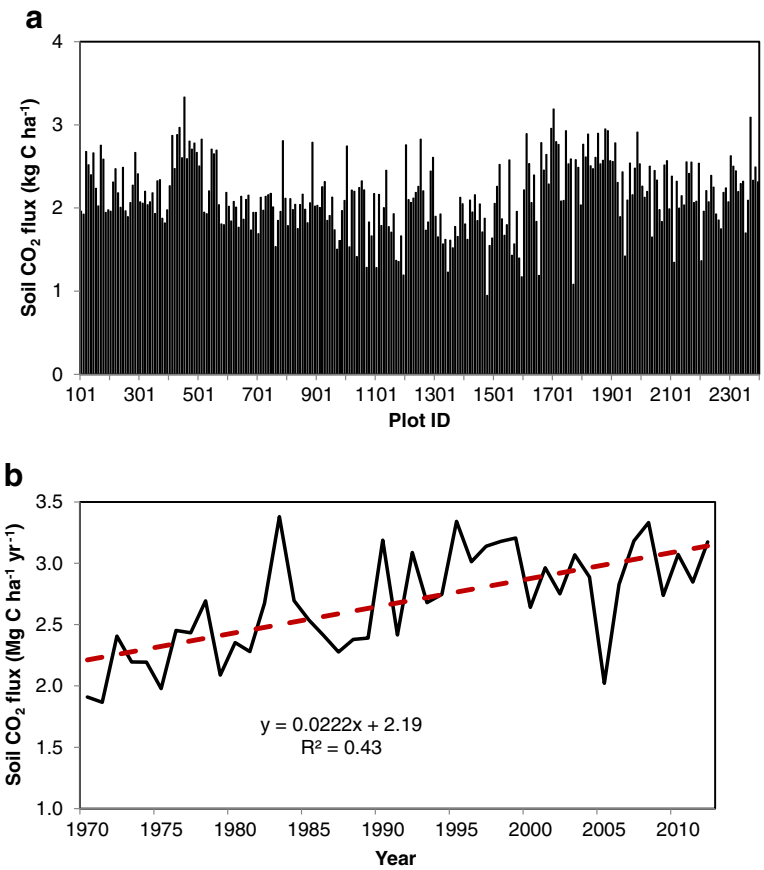

Fig. 6 **a** Soil CO_2 flux from the 276 plots simulated for 2012. **b** The simulated annual soil CO_2 flux for the plot 407 in the period from 1970 to 2012

in 1970 to 19.32 Mg C ha^{-1} in 2012 based on the ratio of root mass to aboveground biomass (Schroth 1995; IPCC 2003). The annual increment in soil CO_2 flux (22.2 kg C ha^{-1} $year^{-1}$) from this plot is similar to rates in a subtropical pine-hardwood forest in South Carolina of USA, about 27 kg C ha^{-1} $year^{-1}$ in a 39-year period from 1950 to 1988 as reported by Dai et al. (2013).

The annual soil CO_2 flux increased with increasing annual precipitation from 1970 to 2012 (R^2=0.43, n= 43, P<0.01), indicating that soil CO_2 flux is significantly regulated by precipitation. The relationship between annual precipitation and soil moisture is consistent with previous findings (Raich and Schlesinger 1992; Amacher and Mackowiak 2011). However, the relationship in this dry semi-deciduous forest is opposite to what has been observed in wet areas, especially in locations near riparian zones, where the annual soil CO_2 flux may decrease with an increase in annual precipitation due to a long soil saturation period and low microbial decomposition (Dai et al. 2013).

3.4 N_2O and CH_4 Fluxes

The soil N_2O flux from the forestland at Kaxil Kiuic varied spatially from 0.26 to 1.77 kg N ha^{-1} in 2012, with a mean of 0.75 kg N ha^{-1}. Similar to soil CO_2 flux, the spatial distribution of the N_2O flux was normal, as indicated by the similarity between the median (0.72 kg N ha^{-1}) and the geometric mean flux. The spatial variability in N_2O flux may be related to variability in soil organic matter (SOM), especially litter that decomposes fast under the tropical climate. The estimated mean N_2O flux can increase by about 0.15 kg N ha^{-1} $year^{-1}$ with an increase in leaf litter at a rate of 2,000 kg ha^{-1} $year^{-1}$. Annual N_2O flux is also associated with annual precipitation due to rain events that are one of the factors driving N_2O emission from soils (Li et al. 1992). Thus, the processes responsible for N_2O flux are related to OM decomposition which releases organic nitrogen and precipitation regulating the processes of nitrification and denitrification in upland ecosystems (Li et al. 1992;

Breuer et al. 2002; Barnard et al. 2006; Lu et al. 2012).

Variability in simulated CH_4 uptake by soils in this forestland was small, ranging from 5.97 to 9.21 kg CH_4–C ha^{-1} in 2012, with a mean of 6.84 kg CH_4–C ha^{-1}. The methane uptake rate by soils in this forest is higher than the rates in a temperate forest in New Hampshire reported by Crill (1991) (4.3–4.6 kg C ha^{-1} $year^{-1}$), in German forests reported by Guckland et al. (2009) (2.0–3.2 kg C ha^{-1} $year^{-1}$), and in Swedish forests found by Klemedtsson and Klemedsson (1997) (0.6–1.6 kg C ha^{-1} $year^{-1}$). However, our rate was similar to or slightly lower than the average methane uptake rate within the 26° N–44° N latitude range in Japan (8.18 kg C ha^{-1} $year^{-1}$) (Ishizuka et al. 2009), within the range in Harvard Forest in Massachusetts found by Steudler et al. (1989) (0–11.57 kg C ha^{-1} $year^{-1}$), and lower than the rate in a subtropical forest in South Carolina observed by Renaud (2008) (6.94–26.65 kg C ha^{-1} $year^{-1}$). Two potential reasons for discrepancies may be the relatively large uncertainties in the estimates of CH_4 uptake and differences in local physiochemical soil properties, because methane uptake by soils is regulated by soil texture, microorganisms, and moisture.

3.5 Spatial Differences in Net Primary Production and Net Ecosystem Production

The simulated net primary production (NPP, consisting of overstory, understory, and ground-growth) using polygons for the forest at Kaxil Kiuic varied little, ranging from 460 to 590 g m^{-2} $year^{-1}$ in 2012 (Fig. 7a). The NPP from the 276 plots simulated for the same year had a greater range from 250 to 800 g m^{-2} $year^{-1}$, but the means of both the plot and polygon simulations were about 510 g m^{-2} $year^{-1}$.

Net ecosystem production (NEP) is an important parameter to assess C sequestration in forest ecosystems. The NEP is defined here as the difference between the net ecosystem exchange (NEE) and the loss of dissolved organic C (DOC) to leachate. The estimated NEP from the simulation using polygons showed that the spatial variation in NEP (range, 219 g m^{-2} $year^{-1}$) was slightly larger than NPP (range, 133 g m^{-2} $year^{-1}$) (Fig. 7b). The slightly larger range in NEP may result from variation in soil and vegetation, leading to differences in autotrophic and heterotrophic respiration and DOC losses to leachate (<3.1 g C m^{-2} $year^{-1}$ on average).

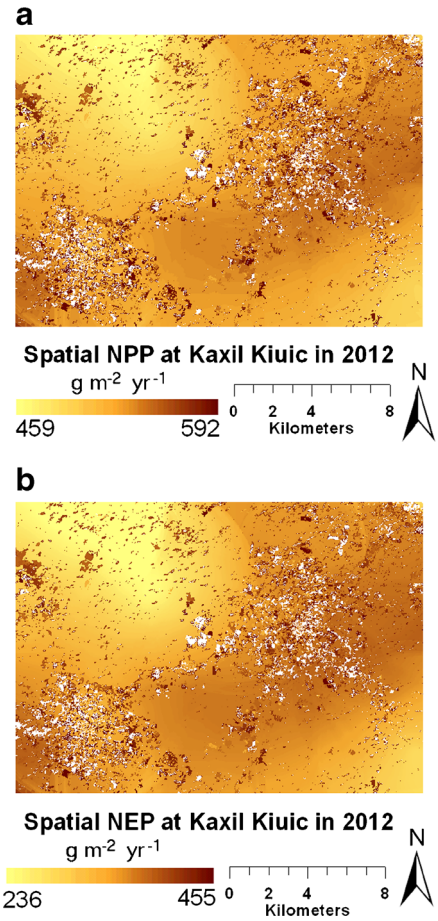

Fig. 7 **a** Spatial net primary production in 2012; the blank (*white*) spots are agricultural and urban areas. **b** Spatial net ecosystem production (NEP) in 2012 in Kaxil Kiuic forest; the blank (*white*) spots are agricultural and urban areas

3.6 Temporal Carbon Dynamics

The validated model was used to assess long-term C dynamics in the Kaxil Kiuic forest for a 150-year period using the 43-year (1970–2012) climate data repeated for the entire modeling period. We assumed that (1) the soil and vegetation types were the same as those currently sampled; (2) woody plants were regenerated in the first year of this 150-year period; (3) the climate over the whole 150-year period followed the observed pattern in the 43-year period. Three variables, annual NPP, NEP, and NEE, were estimated based on the simulation. Annual NEE reached the peak value several years after the tree generation, followed by a long-term decline

(Fig. 8a). This trend in the NEE is similar to the trend in the NPP, but the decline of the NEE is steeper. This steep NEE decline may be due to an increase in respiration, including root respiration and SOM decomposition, since there is no decrease in the GPP in the simulation period (Fig. 8b). The temporal change in the NEE is nonlinear. The fitted equation can be expressed as

$$NEE_{Age} = K_0 \times Age + \sum_{j=1}^{m} K_j \times [\mathrm{In}(\mathrm{Age})]^j \quad (5)$$

where K_0 and K_j are coefficients; *Age* is stand age; m=4. NEE is significantly correlated to stand age (F=117,523.0, P<0.001, and sample number n=150). In contrast to NEE, annual NEP gets slightly smaller as stand age increases. The mean difference in the 150-year period was about 4.22 g m^{-2} $year^{-1}$. The relationship between stand age and NEP is similar to that between NEE and stand age (Eq. 5), but with different coefficients. This small discrepancy between NEP and NEE is presumably due to leaching and occasional surface flow that erodes away C from forest floor and soils.

The relationship between NPP and stand age is presented in Fig. 8b. After reaching peak NPP, there was a slow decrease with stand age, indicating an increase of plant respiration as the stand grew older. The relationship between NPP and stand age based on the simulated results is

$$NPP_{Age} = K_0 \times Age + \sum_{j=1}^{m} K_j \times [\mathrm{In}(Age)]^j \quad (6)$$

where K_0 and K_j are coefficients; Age is stand age; m=5. NPP is significantly correlated with stand age (F=734,985.2, P<0.0001, and n=150).

The relationship between NPP and stand age was similar to that reported for a deciduous broad-leaved community and a mixed forest by He et al. (2012). However, the NPP calculated using the equation suggested by Chen et al. (2003) with specific coefficients for this forest is lower compared with that calculated

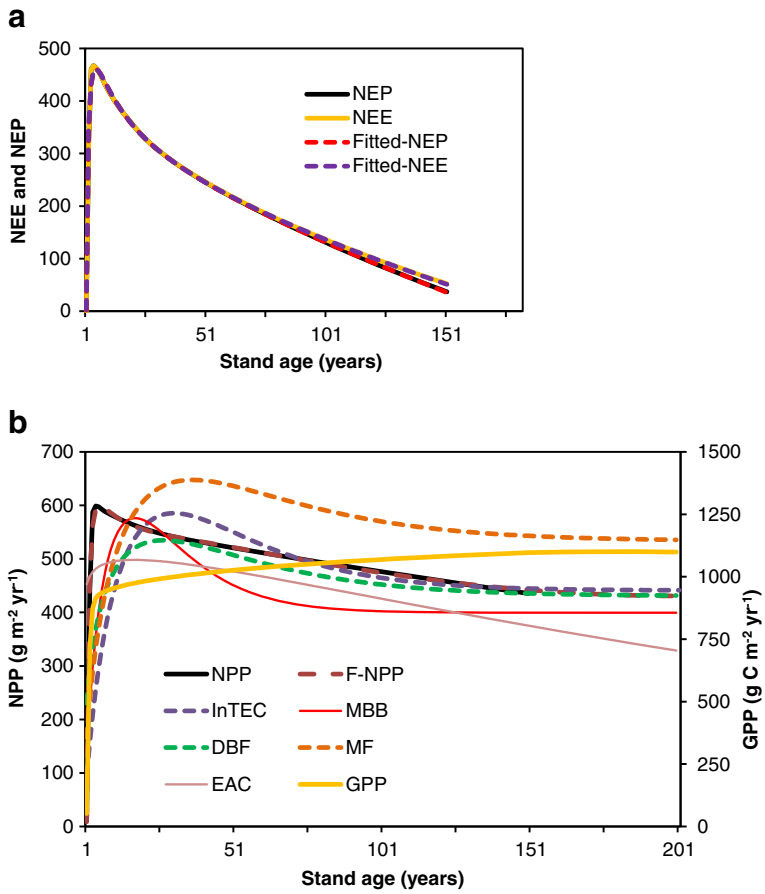

Fig. 8 **a** Temporal changes in annual net ecosystem exchange (*NEE*) (g m^{-2} $year^{-1}$) and annual net ecosystem production (*NEP*) (g m^{-2} $year^{-1}$) in Kaxil Kiuic forest. **b** Temporal changes in annual net primary production (*NPP*) and gross primary production (*GPP*) (g C m^{-2} $year^{-1}$) in Kaxil Kiuic forest compared with estimates from other regions [*GPP* and *NPP* are simulated; *F-NPP* is calculated using Eq. 6 from this study; *InTEC* is calculated using Chen et al. (2003) equation suggested with specific coefficients for this forest; *MBB* maple/beech/birch, *DBF* deciduous broad-leaved forest, *MF* mixed forest, and *EAC* elm/ash/cottonwood are calculated using Chen et al. (2003) equation with He et al. (2012) coefficients]

using Eq. 6 (DNDC) for the period before the stand matures (Fig. 8b). One reason for the disagreement may be that our modeled NPP included contributions from all plants, sedges, understory, and overstory. However, we did not remove those contributions from a non-dominant canopy (or vegetation layers) because non-dominant plants are a part of the entire ecosystem. Moreover, this error becomes small as the forest matures because sedges are small or almost absent, and the understory vegetation can be substantially lower under complete canopy closure.

3.7 Impact of Disturbances on Carbon Stocks

The impact of disturbances on C stocks was investigated by comparing simulations that included and excluded mapped disturbances (see details in Methods and Data). The total disturbed area between 1985 and 2010 was 5,785.5 ha, about 17.5 % of the land. However, the forest area only decreased by 1,227.74 ha, where 21.2 % of the total disturbed area was due to deforestation from agriculture and urbanization development. Accordingly, we estimate that there were about 4,557.7 ha of the land disturbed by forest product harvest and cropland abandonment followed by regenerating forest.

Difference comparison between modeled biomass C with disturbances (1,667.6 Gg C, Fig. 5) and without disturbances (1,822.3 Gg C, Fig. 9) revealed an estimated loss of total biomass C storage of 154.7 Gg C. The mean biomass C storage in the stands would be reduced from 59.9 Mg C ha^{-1} without disturbances to 56.6 Mg C ha^{-1} with disturbances in 2012. The loss of biomass C storage due to conversion of forest to agriculture and urban land use was about 73 Gg C, excluding C loss in dead roots, which was estimated to be 20 Gg C. Accordingly, the estimated total C loss to agriculture and urbanization is about 100 Gg C due only to a loss of about 12 km^2 of the forestland to agriculture and urbanization within this forest in the period from 1985 to 2010, indicating that land use conversion from forest to non-forest can substantially influence C stocks.

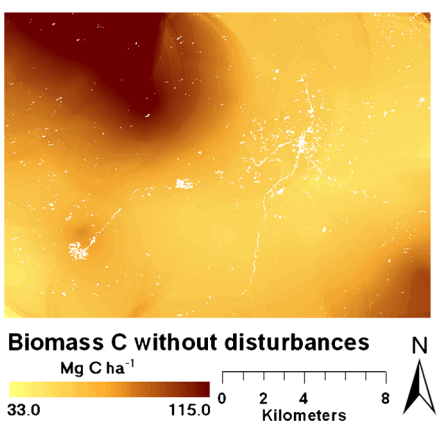

Fig. 9 Simulated spatial biomass carbon distribution for 2012 without disturbances occurred since 1985 in Kaxil Kiuic forest; the blank (*white*) spots are agricultural and urban areas

4 Conclusions

Results from the model evaluation using four quantitative methods and biomass measurements indicate that Forest-DNDC can be used to assess C dynamics for the tropical dry forest at Kaxil Kiuic in the Yucatan Peninsula, Mexico, with a high model performance efficiency (E=0.79, R^2=0.83). The small difference in biomass C stored in the stands between the observation and simulation may be related to inconsistencies between the stand age estimated by interviewing the land users and by using kriging interpolation based on the field data. There are some differences between simulated C stocks using polygonal simulation units and plot measurements due to resolution issues between the plot and polygon sizes. However, this effect does not seem to influence the regional average.

Spatial variability in simulated C stocks reflects variations in stand age, vegetation type, soil characteristics, and disturbance. The disturbances that occurred between 1985 and 2010 led to a mean decrease in C stocks of 3.2 Mg C ha^{-1} in 2012, and a total decrease of about 70 Gg C over 12 km^2 of forestland loss to crops and urban areas. The simulation for long-term C dynamics shows that mean annual NPP, NEE, and NEP change nonlinearly with stand age.

The spatial distributions of soil-borne trace gases, soil CO_2, CH_4, and N_2O, are normal, although spatially explicitly modeled results vary largely. Soil CO_2 flux increases linearly with an increase in precipitation and stand age, while N_2O flux was only associated with precipitation. CH_4 is different from soil CO_2 and N_2O, and uncorrelated with precipitation and stand age.

The results from this study indicate that the spatially explicit process model Forest-DNDC is applicable for modeling C dynamics in the secondary tropical dry

forests with hilly topographic landscape, high species diversity and heterogeneity in disturbances using high resolution inputs. This model can, therefore, be used to provide baseline estimates of C stocks and dynamics to assess or project future human disturbances (e.g., land use changes and forest product harvesting), and evaluate their impact on C dynamics and GHG emissions, and would, therefore, be very useful for the implementation of REDD + initiatives.

Acknowledgments This project was supported by the North American Commission for Environmental Cooperation and the US Agency for International Development. This research was conducted with data from the Mexican network of Intensive Carbon Monitoring Sites (MEX-SMIC). The network is an affiliation of Academic Institutions, Government and NGO investigators with various funding sources. The network currently includes five forested sites located in strategic landscapes for MRV-REDD + activities. Ecosystem C has been estimated using similar protocols since 2012 at various spatial and temporal scales with a variety of methods (e.g., inventory plots, remote sensing, eddy covariance, and ecosystem carbon models). More details can be found at: http://www.mrv.mx/mexsmic. We thank Dr. Jeff Masek of NASA for providing the disturbance map.

References

Amacher, M. C., & Mackowiak, C. L. (2011). Seasonal soil CO_2 flux under Big Sagebrush (*Artemisia tridentata* Nutt.). *Natural Resources and Environmental Issues, 17*, 1–13.

Bauer-Gottwein, P., Gondwe, B. R. N., Charvet, G., Marin, L. E., Rebolledo-Vieyra, M., & Merediz-Alonso, G. (2011). Review: the Yucatan Peninsula karst aquifer, Mexico. *Hydrogeology Journal*. doi:10.1007/s10040-010-0699-5.

Bianchini, E., Pimenta, J. A., & dos Santos, F. A. (2001). Spatial and temporal variation in the canopy cover in a tropical semi-deciduous forest. *Brazilian Archives of Biology and Technology, 44*, 269–276.

Birdsey, R., Pregitzer, K., & Lucier, A. (2006). Forest carbon management in the United States: 1600–2100. *JEQ, 35*, 1461–1469.

Birdsey, R. A., Jenkins, J. C., Johnson, M., Huber-Sannwald, E., Amiro, B., de Jong, B., Barra, J. D. E., French, N., Garcia-Oliva, F., Harmon, M. E., Heath, L. S., Jaramillo, V. J., Johnsen, K., Law, B. E., Marin-Spiotta, E., Masera, O., Neilson, R., Pan, Y., & Pregitzer, K. S. (2007). North American forests. In A. W. King, L. Dilling, G. P. Zimmerman, D. M. Fairman, R. A. Houghton, G. Marland, A. Z. Rose, & T. J. Wilbanks (Eds.), *The first state of the carbon cycle report (SOCCR): the North American carbon budget and implications for the global carbon cycle, a report by the US Climate Change Science Program and the Subcommittee on Global Change Research* (pp. 117–126). Asheville: National Oceanic and Atmospheric Administration, National Climate Data Center.

Barnard, R., Le Roux, X., Hungate, B. A., Cleland, E. E., Blankinship, J. C., Barthes, L., & Leadley, P. W. (2006). Several components of global change alter nitrifying and denitrifying activities in an annual grassland. *Functional Ecology, 20*, 557–564.

Borchert, R., Rivera, G., & Hagnauer, W. (2002). Modification of vegetation phenology in a tropical semi-deciduous forest by abnormal drought and rain. *Biotropica, 34*, 27–39.

Breuer, L., Kiese, R., & Butterbach-Bahl, K. (2002). Temperature and moisture effects on nitrification rates in tropical rain-forest soils. *Soil Science Society of America Journal, 66*, 834–844.

Brown, S., & Lugo, A. E. (1982). The storage and production of organic matter in tropical forests and their role in the global carbon cycle. *Biotropica, 14*, 161–187.

Brown, S., & Lugo, A. E. (1990). Tropical secondary forests. *J Tropical Ecology, 6*, 1–13.

Cairns, M. A., Olmsted, I., Granados, J., & Argaez, J. (2003). Composition and aboveground tree biomass of a dry semi-evergreen forest on Mexico's Yucatan Peninsula. *Forest Ecology and Management, 186*, 125–132.

Charman, D. J., Beilman, D. W., Blaauw, M., Booth, R. K., Brewer, S., Chambers, F. M., Christen, J. A., Gallego-Sala, A., Harrison, S. P., Hughes, P. D. M., Jackson, S. T., Korhola, A. K., Mauquoy, D., Mitchell, F. J. G., Prentice, I. C., van der Linden, M., De Vleeschouwer, F., Yu, Z. C., Alm, J., Bauer, I. E., Corish, Y. M. C., Garneau, M., Hohl, V., Huang, Y., Karofeld, E., Le Roux, G., Loisel, J., Moschen, R., Nichols, J. E., Nieminen, T. M., MacDonald, G. M., Phadtare, N. R., Rausch, N., Dillasoo, U., Swingdles, G. T., Tuittila, E.-S., Ukommaanaho, L., Valiranta, M., van Bellen, S., van Geel, B., Vitt, D. H., & Zhao, Y. (2013). Climate-related changes in peatland carbon accumulation during the millennium. *Biogeosciences, 10*, 929–944. doi:10.5194/bg-10929-2013.

Chen, J. M., Ju, W., Cihlar, J., Price, D., Liu, J., Chen, W., Pan, J., Balck, A., & Barr, A. (2003). Spatial distribution of carbon sources and sinks in Canada's forests. *Tellus, 55B*, 622–641.

Comision Nacional Del Agua (CONAGUA). (2012). Climatic means by station. Accessed November. http://smn.cna.gob.mx/

Crill, P. M. (1991). Seasonal patterns of methane uptake and carbon dioxide release by a temperate woodland soil. *Global Biogeochemical Cycles, 5*, 319–334.

Dai, Z., Amatya, D. M., Sun, G., Trettin, C. C., Li, C., & Li, H. (2011). Climate variability and its impact on forest hydrology on South Carolina coastal plain, USA. *Atmosphere, 2*, 330–357. doi:10.3390/atmos2030330.

Dai, Z., Trettin, C. C., Li, C., Li, H., Sun, G., & Amatya, D. M. (2012). Effect of assessment scale on spatial and temporal variations in CH_4, CO_2 and N_2O fluxes in a forested watershed. *Water, Air, and Soil Pollution, 223*, 253–265. doi:10.1007/s11270-011-0855-0.

Dai, Z., Trettin, C. C., Li, C., Sun, G., Amatya, D. M., & Li, H. (2013). Modeling the impacts of climate variability and hurricane on carbon sequestration in a coastal forested wetland in South Carolina. *Natural Science, 5*, 375–388. doi:10.4236/ns.2013.53051.

Daubenmire, R. (1972). Phenology and other characteristics of tropical semi-deciduous forest in North-Western Costa Rica. *Journal of Ecology, 60*, 147–170.

Dupuy, J. M., Hernandez-Stefanoni, J. L., Hernandez-Juarez, R. A., Tetetia-Rangel, E., Lopez-Martinez, J. O., Leyequien-Abaca, E., Tun-Dzul, F. J., & May-Pat, F. (2012). Patterns

and correlates of tropical dry forest structure and composition in highly replicated chronosequence in Yucatan, Mexico. *Biotropica, 44*, 151–162.

Eaton, J. M., & Lawrence, D. (2008). Loss of carbon sequestration potential after several decades of shifting cultivation in the Southern Yucatan. *Forest Ecology and Management*. doi:10.1016/j.foreco.2008.10.019.

Goward, S. N., Masek, J. G., Cohen, W., Moisen, G., Collatz, G. J., Healey, S., Houghton, R., Huang, C., Kennedy, R., Law, B., Powell, S., Turner, D., & Wulder, M. A. (2008). Forest disturbance and North American carbon flux. *Eos Transactions, 89*, 105–116.

Guckland, A., Flessa, H., & Prenzel, J. (2009). Controls of temporal and spatial variability of methane uptake in soils of a temperate forest with different abundance of European beech (*Fagus sylvatica* L.). *Soil Biology & Biochemistry, 41*, 1659–1667. doi:10.1016/j.soilbio.2009.05.006.

Hansen, J., Sato, M., Ruedy, R., Lo, K., Lea, D. W., & Medina-Elizade, M. (2006). Global temperature change. *Proceedings of the National Academy of Science, 103*, 14288–14293.

Haug, G. H., Gunther, D., Peterson, L. C., Sigman, D. M., Hughen, K. A., & Aeschlimann, B. (2003). Climate and the collapse of Maya civilization. *Science, 299*, 1731–1735.

He, L., Chen, J. M., Pan, Y., Birdsey, R., & Kattge, J. (2012). Relationship between net primay productivity and forest stand age in U.S. forests. *Global Biogeochemical Cycles, 26*, GB3009. doi:10.1029/2010GB003942.

Hernandez-Stefanoni, J. L., Dupuy, J. M., Tun-Dzul, F., & May-Pat, F. (2011). Influence of landscape structure and stand age on species density and biomass of a tropical dry forest across spatial scales. *Landscape Ecology, 26*, 355–370. doi:10.1007/s10980-010-9561-3.

Hodell, D. A., Curtis, J. H., & Brenner, M. (1995). Possible role of climate in the collapse of classic Maya civilization. *Nature, 375*, 391–394.

Holdridge, L. R. (1967). *Life zone ecology*. San Jose: Tropical Science Center. 206pp.

Hughes, R. F., Kauffman, J. B., & Jaramillo, V. J. (1999). Biomass, carbon, and nutrient dynamics of secondary forests in a humid tropical region of Mexico. *Ecology, 80*, 1892–1907.

IPCC. (2003). Chapter 3. In J. Penman, M. Gytarsky, T. Hiraishi, T. Krug, D. Kruger, R. Pipatti, L. Buendia, K. Miwa, T. Ngara, K. Tanabe, & F. Wagner (Eds.), *Good practice guidance for land use, land-use change and forestry* (pp. 3.1–3.150). Kanagawa: IPCC.

IPCC. (2007). *Climate change 2007*: The physical science basis. Contribution of working group I to the fourth assessment report of the intergovernmental panel on climate change. In: Solomon, S., Qin, D., Manning, M., Chen, Z., Marquis, M., Averyt, K.B., Tignor, M., and Miller, H.L. (Eds). Paris, France, February 2007.

Ishizuka, S., Sakata, T., Sawata, S., Ikeda, S., Sakai, H., Takenaka, C., Tamai, N., Onodera, S., Shimizu, T., Kan-na, K., Tanaka, N., & Takahashi, M. (2009). Methane uptake rates in Japanese forest soils depend on the oxidation ability of topsoil, with a new estimate for global methane uptake in temperate forest. *Biogeochemistry, 92*, 281–295. doi:10.1007/s10533-009-9293-0.

Jassim, F. A., & Altaany, F. H. (2013). Image interpolation using kriging technique for spatial data. *Canadian Journal of Image Proceeding and Computer Vision, 4*, 16–21.

Kato, T., Knorr, W., Schoize, M., Veenendaal, E., Kaminski, T., Kattge, J., & Gobron, N. (2013). Simultaneous assimilation of satellite and eddy covariance data for improving terrestrial water and carbon simulations at a semi-arid woodland site in Botswana. *Biogeosciences, 10*, 789–802. doi:10.5194/bg-10-789-2013.

Kennard, D. K., Gould, K., Putz, F. E., Fredericksen, T. S., & Morales, F. (2002). Effect of disturbance intensity on regeneration mechanisms in a tropical dry forest. *Forest Ecology and Management, 162*, 197–208.

Kesik, M., Bruggemann, N., Forkel, R., Kiese, R., Knoche, R., Li, C., Seufert, G., Simpson, D., & Butterbach-Bahl, K. (2006). Future scenarios of N2O and NO emissions from European forest soils. *Journal of Geophysical Research, 111*, G02018. doi:10.1029/2005JG000115.

Kiese, R., Li, C., Hilbert, D. W., Papen, H., & Butterbach-Bahl, K. (2005). Regional application of PnET-DNDC for estimating the N2O source strength of tropical rainforests in the Wet Tropics of Australia. *Global Change Biology, 11*, 128–144.

Klemedtsson, A. K., & Klemedtsson, L. (1997). Methane uptake in Swedish forest soil in relation to liming and extra N-deposition. *Biology and Fertility of Soils, 25*, 296–301.

Kurbatova, J., Li, C., Varlagin, A., Xiao, X., & Vygodskaya, N. (2008). Modeling carbon dynamics in two adjacent spruce forests with different soil conditions in Russia. *Biogeosciences, 5*, 969–980.

Li, C., Frolking, S., & Frolking, T. A. (1992). A model of Nitrous oxide evolution from soil driven by rainfall events: 2. Model applications. *JGR, 97*, 9777–9783.

Li, C., Aber, J., Stang, F., Butter-Bahl, K., & Papen, H. (2000). A process-oriented model of N_2O and NO emissions from forest soils. 1. Model development. *Journal of Geophysical Research Atmospheres, 105*, 4369–4384.

Li, C., Cui, J., Sun, G., & Trettin, C. C. (2004). Modeling impacts of management on carbon sequestration and trace gas emissions in forested wetland ecosystems. *Environmental Management (Supplement), 33*, S176–S186.

Li, J. & Heap, A.D. (2008). A review of spatial interpolation methods for environmental scientists. Geoscience Australia, Record 2008/23, pp137, ISSN 1448–2177, Canberra, Australia.

Lu, X., Yan, Y., Fan, J., & Wang, X. (2012). Gross nitrification and denitrification in alpine grassland ecosystems on the Tibetan Plateau. *Actic, Antarctic, and Alpine Research, 44*, 188–196.

Miehle, P., Livesley, S. J., Feikema, P. M., Li, C., & Arndt, S. K. (2006). Assessing productivity and carbon sequestration capacity of Eucalyptus globules plantation using the process model Forest-DNDC: calibration and validation. *Ecological Modeling, 192*, 83–94.

Moriasi, D., Arnold, J., Liew, M. W. V., Bingner, R., Harmel, R., & Veith, T. (2007). Model evaluation guidelines for systematic quantification of accuracy in watershed simulations. *ASABE, 50*, 885–899.

Nash, J. E., & Sutcliffe, J. V. (1970). River flow forecasting through conceptual models-part I: a discussion of principles. *Journal of Hydrology, 10*, 282–290.

Pacific, V. J., McGlynn, B. L., Riveros-Iregui, D. A., Epstein, H. E., & Welsch, D. L. (2009). Differential soil respiration response to changing hydrologic regimes. *Water Resources Research, 45*, W07201. doi:10.1029/2009WR007721.

Pan, Y., Birdsey, R. A., Fang, J., Hounghton, R., Kauppi, P. E., Kurz, W. A., Phillips, O. L., Shvidenko, A., Lewis, S. L., Ganadell, J. G., Ciais, P., Jackson, R. B., Pacala, S. W., McGuire, D., Piao, S., Rautiainen, A., Sitch, S., & Hayes, D. (2011). A large and persistent carbon sink in the world's forests. *Science, 333*, 988–993. doi:10.1126/science.1201609.

Pietsch, S. A., Hasenauer, H., Kucera, J., & Cermak, J. (2003). Modeling effects of hydrological changes on the carbon and nitrogen balance of oak in floodplains. *Tree Physics, 23*, 735–746.

Raich, J. W., & Schlesinger, W. H. (1992). The global carbon dioxide flux in soil respiration and its relationship to vegetation and climate. *Tellus, 44B*, 81–99.

Read, L., & Lawrence, D. (2003). Recovery of biomass following cultivation in dry tropical forests of the Yucatan. *Ecological Application, 13*, 85–97.

Renaud, L. (2008). *Methane emissions from bottomland hardwood wetlands in Francis Marion National Forest, SC* (p. 112). Charleston: College of Charleston.

Rico-Gray, V., & Garcia-Franco, J. G. (1991). The Maya and the vegetation of the Yucatan peninsula. *Journal of Ethnobiology, 11*, 135–142.

Riveros-Iregui, D. A., & McGlynn, B. L. (2009). Landscape structure control on soil CO_2 efflux variability in complex terrain: scaling from point observation to watershed scale fluxes. *Journal of Geophysical Research, 114*, G02010. doi: 10.1029/2008JG000885.

Ryan, M.G. (2008). Forests and carbon storage (June 4, 2008), U.S. Department of Agriculture, Forest Service, Feb. 8, 2013. http://www.fs.fed.us/ccrc/topics/carbon.shtml.

Schroth, G. (1995). Tree root characteristics as criteria for species selection and systems design in agroforestry. *Agroforestry Systems, 30*, 125–143. doi:10.1007/BF00708917.

Stange, F., Butterbachl, K., Papen, H., Zechmeister-Boltenstern, S., Li, C., & Aber, J. (2000). A process-oriented model of N_2O and NO emissions from forest soils. *Journal of Geophysical Research, 105*, 4385–4398.

Steudler, P. A., Bowden, R. D., Melillo, J. M., & Aber, J. D. (1989). Influence of nitrogen fertilization on methane uptake in temperate forest soils. *Nature, 341*, 314–316.

Trettin, C. C., Laiho, R., Minkkinen, K., & Laine, J. (2006). Influence of climate change factors on carbon dynamics in northern forested peatlands. *Canadian Journal of Soil Science, 86*, 269–280.

Turner, B. L., II, Cortina-Villar, S., Forester, D., Geoghegan, J., Keys, E., Klepeis, P., Lawrence, D., Macario Mendoza, P., Manson, S., Ogneva-Himmelberger, Y., Plotkin, A. B., Perez-Salicrup, D., Roy-Chowdhury, R., Savitsky, B., Schneider, L., Schmook, B., & Vance, C. (2001). Deforestation in the southern Yucatan peninsula region: an integrative approach. *Forest Ecology and Management, 154*, 353–370.

Zhang, Y., Li, C., Trettin, C. C., Li, H., & Sun, G. (2002). An integrated model of soil, hydrology and vegetation for carbon dynamics in wetland ecosystems. *Global Biogeochemical Cycles, 16*, GB001838. doi:10.1029/2001.